(6); MS (ESI$^+$): m/z (relative intensity): 873.5 (10) [M+H$^+$], 813.5 (100) [M+H$^+$ − CH_3COOH]. MS (DCI/NH_3^+): m/z: (relative intensity) 873 (2) [M+H$^+$], 816 (6), 815 (20), 814 (52), 813 (100) [M+H$^+$ − CH_3COOH], 812 (4); ^{1}H NMR (400.13 MHz, $CDCl_3$, for clarity, the signals of the porphyrin moiety are described first, and then those of the artemisinin fragment): δ = 10.23, 10.17, 10.14, 10.07, 10.05, 10.01, 9.96, 9.90, 9.82 (9 × s, 3H, *meso*-H), 8.29, 8.24, 8.18, 8.16, 8.05, 8.07 (6 × m, 2H, H_c), 6.39, 6.30, 6.31, 6.20, 6.16, 5.94 (4H, H_a and H_b), 4.37 (m, 4H, H_2C-C13′ and H_2C-C17′), 3.75 – 3.57 (18H, H_3C-C2′, H_3C-C7′, H_3C-C12′, H_3C-C18′, and COOCH_3), 3.25 (m, 4H, $H_2CCOOCH_3$), −2.79 (2H, NH), 5.45 and 5.15 (2 × m, 2 × H, H_2C4), 2.07, 1.77, 1.56 (H_2C5), 1.11 and 0.58 (H5a), 1.28 (m, 1H, H6), 0.92 (d, 3H, ^3J = 6 Hz, H_3C-C6), 1.98 and 1.51 (H_2C7), 1.93 and 0.98 (H_2C8), 2.06 (H8a), 3.21 (m, 1H, H9), 1.22 (d, 3H, ^3J = 7 Hz, H_3C-C9), 5.60 (s, 1H, H12), 1.59 (s, 3H, H_3CCOO-C12), 1.53 (*H*O-C12a).

Analytical HPLC conditions: column: C8 on Lichrosorb 10 μm (Interchrom, France); eluent A: 0.1 vol% aqueous trifluoracetic acid, eluent B: CH_3CN; gradient program: linear from 40% to 70% of eluent B for 50 min, then linear from 70% to 100% of B for the following 15 min, 1 mL min^{-1}; products were detected at λ = 420 nm to follow the modifications of the porphyrin chromophore. To monitor the reaction, aliquots (50 μL) were evaporated to dryness, dissolved in a mixture (1 mL, 1:1, v/v) of acetonitrile and aqueous trifluoroacetic acid (0.1 vol%), and analyzed (injected volume: 100 μL). After 20 – 30 min of reaction time, the conversion of starting hemin (retention time = 26.6 min) was 85 – 90%. Two broad peaks of modified hemin derivatives were detected (retention time = 32.3, 33.1 min, respectively; ESI-MS: m/z: 926.5 [M^+] for this mixture and for each of the two broad peaks recovered after semi-preparative HPLC.

Received: January 17, 2001 [Z16443]

[1] N. J. White, F. Nosten, S. Looareesuwan, W. M. Watkins, K. Marsh, R. W. Snow, G. Kokwaro, J. Ouma, T. T. Hien, M. E. Molyneux, T. E. Traylor, C. I. Newbold, T. K. Ruebush, M. Danis, B. M. Greenwood, R. M. Anderson, P. Olliaro, *Lancet* **1999**, *353*, 1965 – 1967.

[2] S. Pagola, P. W. Stephens, D. S. Bohle, A. D. Kosar, S. K. Madsen, *Nature* **2000**, *404*, 307 – 310.

[3] S. R. Meshnick, T. E. Taylor, S. Kamchonwongpaisan, *Microbiol. Rev.* **1996**, *60*, 301 – 315.

[4] J. N. Cumming, P. Ploypradith, G. H. Posner, *Adv. Pharmacol.* **1997**, *37*, 253 – 297.

[5] A. Robert, B. Meunier, *Chem. Soc. Rev.* **1998**, *27*, 273 – 279.

[6] W. Asawamahasakda, I. Ittarat, Y.-M. Pu, H. Ziffer, S. R. Meshnick, *Antimicrob. Agents Chemother.* **1994**, *38*, 1854 – 1858.

[7] Y.-L. Hong, Y.-Z. Yang, S. R. Meshnick, *Mol. Biochem. Parasitol.* **1994**, *63*, 121 – 128.

[8] A. Robert, B. Meunier, *J. Am. Chem. Soc.* **1997**, *119*, 5968 – 5969.

[9] A. Robert, B. Meunier, *Chem. Eur. J.* **1998**, *4*, 1287 – 1296.

[10] G. H. Posner, C. H. Oh, D. Wang, L. Gerena, W. K. Milhous, S. R. Meshnick, W. Asawamahasakda, *J. Med. Chem.* **1994**, *37*, 1256 – 1258.

[11] J.-H. Fuhrhop, K. M. Smith in *Porphyrins and Metalloporphyrins* (Ed.: K. M. Smith), Elsevier, Amsterdam, **1975**, pp. 757 – 869.

[12] H. Scheer, J. J. Katz in *Porphyrins and Metalloporphyrins* (Ed.: K. M. Smith), Elsevier, Amsterdam, **1975**, pp. 399 – 524.

[13] A. V. Pandey, B. L. Tekwani, R. L. Singh, V. S. Chauhan, *J. Biol. Chem.* **1999**, *274*, 19383 – 19388.

[14] P. Bigey, S. Frau, C. Loup, C. Claparols, J. Bernadou, B. Meunier, *Bull. Soc. Chim. Fr.* **1996**, *133*, 679 – 689.

Assembly of Ni_7 and Ni_{21} Molecular Clusters by Using Citric Acid**

Mark Murrie, Helen Stoeckli-Evans, and Hans U. Güdel*

Exploration of the middle ground between simple molecular species and infinite arrays has led to the discovery of novel, nanoscale materials in the field of molecular magnetism. Single Molecule Magnets (SMM)[1] offer the possibility of information storage at the molecular level, and have provided the first examples in which novel phenomena such as quantum-mechanical tunneling of magnetization can be observed.[2] It is now understood that a large spin ground state (S) and a negative axial anisotropy (D) are a prerequisite.

However, there is a perceived need to develop synthetic approaches to larger, more complex molecules to establish further the relationship between structure and molecular properties. By utilizing simple organic ligands, such as carboxylates, it has been possible to isolate clusters containing up to 24 transition metal ions.[3] The use of more complex ligands such as polycarboxylates[4] or polyalcohols,[5] has been more limited. Polydentate ligands should produce new cluster topologies by virtue of their coordinative flexibility.

We have chosen to investigate the proligand citric acid ($HOC(CO_2H)(CH_2CO_2H)_2$; H_4cit) which has been little employed in cluster synthesis; only two high nuclearity ($N \geq 6$) transition metal citrate complexes are structurally characterized.[6] Nevertheless, we have found that citrate displays a rich solution chemistry with Ni^{II} units and herein report our first success in isolation of two new citrate clusters containing seven and an unprecedented 21 Ni^{II} ions, respectively.

The reaction of Ni^{II} with citrate in basic aqueous solution in the presence of Na^+ and NMe_4^+ ions, followed by the addition of ethanol as cosolvent gives the {Ni_7} cluster **1** (see Experimental Section). The high solubility of such species in aqueous solution makes crystallization by slow evaporation difficult, as previously noted.[6a] We have addressed this problem by adjusting solvent polarity to effect crystallization, thus removing the need for crystallization from highly concentrated, and often viscous solutions. The single crystal X-ray structure of **1** (Figure 1) shows a cluster containing two {Ni_3} trimers related by a pseudo two-fold axis passing through the central Ni (Ni4).[7] The coordination sites at the nickel centers are occupied by the oxygen atoms from the six citrate ligands, apart from a site on both Ni3 and Ni5, which is filled

[*] Prof. Dr. H. U. Güdel, Dr. M. Murrie
Departement für Chemie und Biochemie
Universität Bern
Freiestrasse 3, 3000 Bern 9 (Switzerland)
Fax: (+41) 31-631-4399
E-mail: hans-ulrich.guedel@iac.unibe.ch
Prof. Dr. H. Stoeckli-Evans
Institut de Chimie
Université de Neuchâtel
Avenue de Bellevaux 51, 2000 Neuchâtel (Switzerland)

[**] This work was supported by the Swiss National Science Foundation.

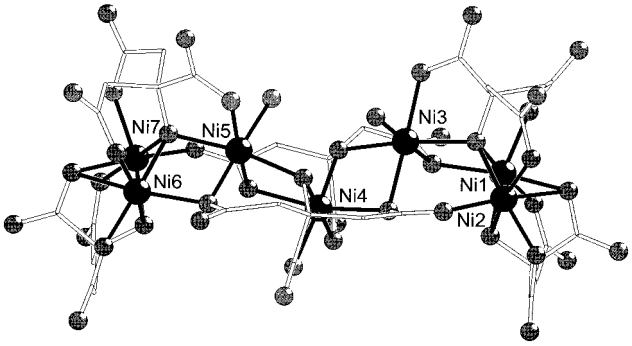

Figure 1. The molecular structure of **1**, H atoms have been omitted for clarity (Ni = black sphere; O = gray sphere; C = rods). Bond length ranges [Å; average esd 0.003 Å] Ni–O: 1.981–2.059 (citrate O^-), 1.998–2.258 (citrate CO_2^-); bond angle ranges [°; average esd 0.1°]: *cis* at Ni 71.0–104.3, *trans* at Ni 161.4–178.1.

by a water molecule. Geometric constraints imposed by the citrate ligands lead to a distorted octahedral nickel coordination environment. The three independent citrate ligands are tetradeprotonated, each utilizing all four binding groups, bridging two (e.g. Ni1 and Ni2), three (e.g. Ni1, Ni2, and Ni3), and five (e.g. Ni1, Ni3, Ni4, Ni5, and Ni7) metal centers. The Na^+ and NMe_4^+ ions in the lattice provide charge balance of the decanionic cluster.

$[Ni_7(cit)_6(H_2O)_2]Na_5(NMe_4)_5$ **1**

The magnetic properties of **1** are interesting: a plot of χT versus T reveals an overall weak ferromagnetic coupling within the $\{Ni_7\}$ cluster (Figure 2; the spin Hamiltonian is given

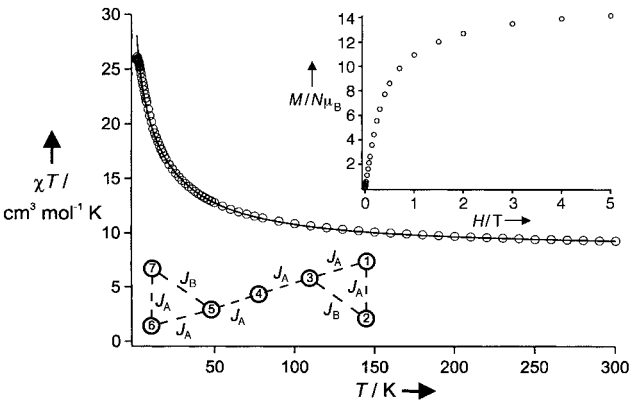

Figure 2. Temperature dependence of χT for **1**. The solid line represents a model using the two different parameters J_A and J_B as follows: $J_A = J_{12} = J_{13} = J_{34} = J_{45} = J_{56} = J_{67}$ and $J_B = J_{23} = J_{57}$. Inset shows the field dependence of the magnetization at 1.8 K.

in Equation (1)).[8] Curie–Weiss behavior is observed above 100 K with a Weiss constant $\theta = 21.8$ K. We attempted to model the data using the simplest possible coupling scheme. Using only one J parameter is clearly inadequate, and two exchange parameters are required to model the data satisfactorily yielding values of $J_A = 10$ and $J_B = -4.5$ cm^{-1} with $g = 2.2$ (see Figure 2).[9] The signs of J_A and J_B can be correlated with the Ni-Ô-Ni bridging angles; the bridging angle for the interaction J_B is 119° while the remaining angles corresponding to J_A are all less than 102°, consistent with antiferro- and ferromagnetic exchange, respectively.[10] The magnitude of the exchange parameters is consistent with that observed for other polynuclear oxo-bridged Ni^{II} complexes.[10b] Furthermore, the model shows good agreement to low temperature without the inclusion of anisotropy, suggesting that any zero-field splitting effects are small.

$$\mathcal{H} = -2J_A(\hat{S}_1\hat{S}_2 + \hat{S}_1\hat{S}_3 + \hat{S}_3\hat{S}_4 + \hat{S}_4\hat{S}_5 + \hat{S}_5\hat{S}_6 + \hat{S}_6\hat{S}_7) - 2J_B(\hat{S}_2\hat{S}_3 + \hat{S}_5\hat{S}_7) \quad (1)$$

The spin ground state is confirmed as $S = 7$ by magnetization measurements at 1.8 K in fields up to 5 T; the magnetization is not saturated at 5 T giving a value of $M/N\mu_B = 14.2$ (calculated 15.4 for $S = 7$ and $g = 2.2$). The simple model used above shows a small exchange splitting of around 1 K between the $S = 7$ energy level and the lowest lying $S = 6$ level. Therefore, at 1.8 K the available thermal energy is significant compared with the exchange splitting and the ground state is not energetically isolated. No out of phase alternating current (ac) signal is observed between 1.8 and 10 K; although **1** has a large spin ground state it possesses nonaxial symmetry, which is not ideal for the observation of SMM properties.

We have found that it is possible to selectively crystallize a further cluster from the reaction mixture by adjusting the amount of cosolvent. Using less ethanol, **1** appears sufficiently soluble to prevent its crystallization, permitting isolation of pure samples of **2**. Single crystal X-ray analysis (Figure 3)

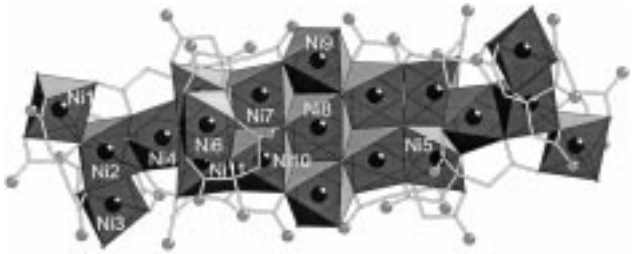

Figure 3. The structure of **2** (polyhedral representation) the H atoms have been omitted for clarity (Ni = black spheres; O = gray spheres; C = rods). Bond length ranges [Å; average esd 0.003 Å] Ni–O: 1.969–2.128 (citrate O^-), 1.997–2.210 (citrate CO_2^-). Bond angle ranges [°; average esd 0.1°]: *cis* at Ni 76.1–106.1, *trans* at Ni 158.65–180.0.

reveals an unusual complex containing 21 Ni^{II} ions; the molecule possesses a center of symmetry at the Ni8 position.[7] Nickel ions have been assigned as Ni^{II} centers and the 10 bridging oxygen atoms as hydroxides (calculated valence 1.09–1.13), on the basis of bond valence sum analysis.[11] The central $\{Ni_7(\mu_3\text{-}OH)_6\}$ core possesses a hexagonal close-packed layer structure as found for $Ni(OH)_2$. This is similar to the $\{Fe_7(\mu_3\text{-}OH)_6\}$ core seen in $\{Fe_{17}\}$ and $\{Fe_{19}\}$ clusters[4a] and portions of a $\{Co_{24}\}$ cluster.[3a] Four of the six edges of the $\{Ni_7(\mu_3\text{-}OH)_6\}$ core are bridged by citrate carboxylate groups; additional ligand binding sites permit cluster growth outside the core. As constraints imposed by the ligands begin to dictate the structure the $Ni(OH)_2$ lattice is no longer preserved leading to the unusual structure in Figure 3. Five

  0044-8249/01/11310-2012 $ 17.50+.50/0

different ligand binding modes are seen with four of these previously unobserved in nickel citrate chemistry.

$[Ni_{21}(cit)_{12}(OH)_{10}(H_2O)_{10}]Na_8(NMe_4)_8$ **2**

A preliminary investigation of the magnetic properties of **2** has been performed; a plot of χT versus T reveals a dominant antiferromagnetic interaction within the cluster (Figure 4).

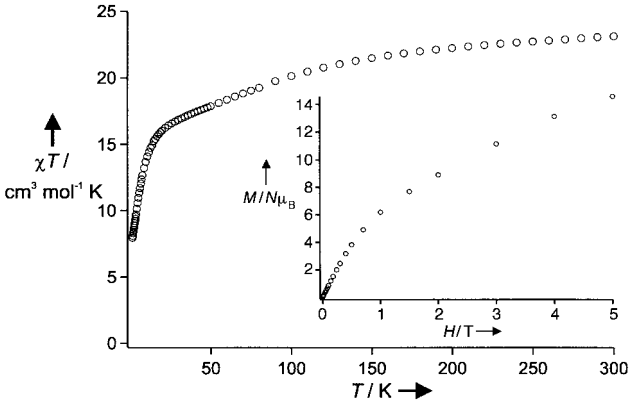

Figure 4. Temperature dependence of χT for **2**. Inset shows the field dependence of the magnetization at 1.8 K.

Curie–Weiss behavior is observed above 100 K with a Weiss constant $\theta = -24.2$ K. Below 100 K the shape of the curve implies a complicated energy-level scheme although the size of the cluster prevents modeling of the data. The exact nature of the spin ground state is difficult to obtain; the value of χT at 1.8 K suggests a spin ground state of around $S = 3$, whereas magnetization data at 1.8 K in a field of 5 T suggest that M_s levels of higher spin states are populated (Figure 4 inset).

The chemistry of citrate with Ni^{II} units in basic aqueous solution appears both fascinating and highly complicated. This study represents only a small reaction parameter space and, by careful modification of the crystallization process, has already yielded two new complexes displaying different structural and completely different magnetic properties. The ligand cit^{4-} shows a binding flexibility towards Ni^{II} centers, displaying seven different coordination modes across the two complexes, bridging up to five metal centers.

Neither of the clusters isolated exhibits SMM properties; even in **1** where a large spin ground state is present the cluster symmetry is nonaxial, reducing the possibility of observing SMM behavior. Nonetheless, it is entirely possible that further clusters are present in such solutions with their formation and crystallization governed by a number of variables. We are currently widening this study in the hope of understanding the factors that dictate the cluster assembly process.

Experimental Section

Addition of an aqueous solution (15 mL) of NaOH (3.520 g, 88.0 mmol) to an aqueous solution (25 mL) of $NiSO_4 \cdot 6H_2O$ (10.907 g, 41.5 mmol) gave a pale green precipitate, which was collected by filtration and washed with distilled water (3 × 100 mL). Dissolution of this solid in an aqueous solution (20 mL) of citric acid monohydrate (7.985 g, 38.0 mmol) gave a solution of pH 2.94. The pH was raised to 9.20 by the addition of $NMe_4OH \cdot 5H_2O$ (12.50 g, 69.0 mmol) and the aqueous solution concentrated to a volume of 35 mL. Aliquots of this solution were taken, mixed with EtOH, and kept in sealed sample tubes (the volumes of EtOH given below permit isolation of pure samples of either **1** or **2**). After one week, well-formed rod-like crystals of **1** could be isolated from solutions of composition: aqueous solution (0.4 mL) and EtOH (either 0.9, 1.0, or 1.1 mL). The crystals were dried under vacuum. Yield per 0.4 mL: 30 mg (17% based on Ni); elemental analysis calcd (%) for $C_{56}H_{148}N_5Na_5Ni_7O_{74}$ ($\mathbf{1} \cdot 30H_2O$): C 25.85, H 5.73, N 2.69; found: C 25.84, H 5.54, N 2.65. After one month, rhomboid crystals of **2** could be isolated from solutions of composition: aqueous solution (0.4 mL) and EtOH (either 0.7 or 0.8 mL). The crystals were dried under vacuum. Yield per 0.4 mL: 10 mg (3% based on Ni); elemental analysis calcd (%) for $C_{108}H_{250}N_8Na_8Ni_{21}O_{138}$ ($\mathbf{2} \cdot 32H_2O \cdot 2EtOH$): C 24.54, H 4.77, N 2.12; found: C 24.43, H 4.83, N 2.24.

Received: January 18, 2001 [Z16454]

[1] a) R. Sessoli, D. Gatteschi, A. Caneschi, M. A. Novak, *Nature* **1993**, *365*, 141–143; b) R. Sessoli, H.-L. Tsai, A. R. Schake, S. Wang, J. B. Vincent, K. Folting, D. Gatteschi, G. Christou, D. N. Hendrickson, *J. Am. Chem. Soc.* **1993**, *115*, 1804–1816.

[2] a) J. R. Friedman, M. P. Sarachick, J. Tejada, R. Ziolo, *Phys. Rev. Lett.* **1996**, *76*, 3830–3833; b) L. Thomas, F. Lionti, R. Ballou, D. Gatteschi, R. Sessoli, B. Barbara, *Nature* **1996**, *383*, 145–147; c) C. Sangregorio, T. Ohm, C. Paulsen, R. Sessoli, D. Gatteschi, *Phys. Rev. Lett.* **1997**, *78*, 4645–4648.

[3] a) E. K. Brechin, S. G. Harris, A. Harrison, S. Parsons, G. Whittaker, R. E. P. Winpenny, *Chem. Commun.* **1997**, 653–654; b) A. L. Dearden, S. Parsons, R. E. P. Winpenny, *Angew. Chem.* **2001**, *113*, 156–158; *Angew. Chem. Int. Ed.* **2001**, *40*, 151–154.

[4] a) S. L. Heath, A. K. Powell, *Angew. Chem.* **1992**, *104*, 191; *Angew. Chem. Int. Ed. Engl.* **1992**, *31*, 191–193; b) S. P. Watton, P. Fuhrmann, L. E. Pence, A. Caneschi, A. Cornia, G. L. Abbati, S. J. Lippard, *Angew. Chem.* **1997**, *109*, 2917–2919; *Angew. Chem. Int. Ed.* **1997**, *36*, 2774–2776; c) R. C. Squire, S. M. J. Aubin, K. Folting, W. E. Streib, G. Christou, D. N. Hendrickson, *Inorg. Chem.* **1995**, *34*, 6463.

[5] a) P. Klüfers, J. Schuhmacher, *Angew. Chem.* **1995**, *107*, 2290–2292; *Angew. Chem. Int. Ed.* **1995**, *34*, 2119–2121; b) J. Burger, P. Klüfers, *Angew. Chem.* **1997**, *109*, 801–804; *Angew. Chem. Int. Ed.* **1997**, *36*, 776–779.

[6] a) J. Strouse, S. W. Layten, C. E. Strouse, *J. Am. Chem. Soc.* **1977**, *99*, 562–572; b) A. Bino, I. Shweky, S. Cohen, E. R. Bauminger, S. J. Lippard, *Inorg. Chem.* **1998**, *37*, 5168.

[7] Crystal data for **1**: Crystal dimensions $0.50 \times 0.50 \times 0.30$ mm; $C_{56}H_{163}N_5Na_4Ni_7O_{83.5}$, $M_r = 2745.84$; triclinic, space group $P\bar{1}$, $a = 13.3224(10)$, $b = 14.5053(11)$, $c = 32.328(2)$ Å, $\alpha = 78.118(9)$, $\beta = 87.006(9)$, $\gamma = 70.951(8)^\circ$, $V = 5777.8(8)$ Å^3, $Z = 2$, $\rho_{calcd} = 1.578$ g cm^{-3}, $T = 153(2)$ K, $2.05^\circ < \theta < 25.90^\circ$; $F(000) = 2884$. Refinement by full-matrix least-squares methods gave final $R1(F_o) = 0.0478$, $wR2(F_o^2) = 0.1340$ for 15974 reflections with $I > 2\sigma(I)$ and 1061 parameters; $R1 = 0.0639$ (all data); max./min. residual electron density 1.193/ −0.922 e Å^{-3}. Crystal data for **2**: Crystal dimensions $0.45 \times 0.40 \times 0.30$ mm; $C_{128}H_{396}N_6Na_2Ni_{21}O_{200}$, $M_r = 6499.40$; triclinic, space group $P\bar{1}$, $a = 19.2254(14)$, $b = 19.5486(14)$, $c = 20.8916(16)$ Å, $\alpha = 67.350(8)$, $\beta = 79.186(9)$, $\gamma = 64.164(8)^\circ$, $V = 6497.5(8)$ Å^3, $Z = 1$, $\rho_{calcd} = 1.661$ g cm^{-3}, $T = 153(2)$ K, $2.05^\circ < \theta < 25.90^\circ$; $F(000) = 3416$. Refinement by full-matrix least-squares methods gave final $R1(F_o) = 0.0546$, $wR2(F_o^2) = 0.1499$ for 23446 reflections with $I > 2\sigma(I)$ and 1053 parameters; $R1 = 0.0810$ (all data); max./min. residual electron density 1.101/ −1.276 e Å^{-3}. Intensity data were collected on a Stoe Image Plate Diffraction system using graphite-monochromated $Mo_{K\alpha}$ radiation ($\lambda = 0.71073$ Å). Image plate distance 70 mm, ϕ oscillation scans 0–200°, step $\Delta\phi = 1^\circ$, 2θ range 3.27–52.1°, d_{max}-d_{min} = 12.45–0.81 Å. Structures were solved by direct methods using the programme SHELXS-97. The refinement and all further calculations were carried out using SHELXL-97. The hydrogen atoms were included in calculated positions and treated as riding atoms using SHELXL-97 default parameters. The non-hydrogen atoms were refined anisotropically, using weighted full-matrix least-squares on F^2. For **1**, because of a large amount of disordered solvent it was impossible to locate correctly entire molecules of ethanol. Hence, it

was assumed that there were 39.5 water molecules present in all, which filled the space available for solvent. For both **1** and **2** it was not possible to locate all cations because of the large amount of disordered solvent present. Charge balance requires a total of ten cations for **1** and sixteen for **2**; the relative proportions of missing Na^+ and NMe_4^+ have been assigned on the basis of microanalysis results. Crystallographic data (excluding structure factors) for the structures reported in this paper have been deposited with the Cambridge Crystallographic Data Centre as supplementary publication no. CCDC-155973 (**1**) and -155972 (**2**). Copies of the data can be obtained free of charge on application to CCDC, 12 Union Road, Cambridge CB2 1EZ, UK (fax: (+44) 1223-336-033; e-mail: deposit@ccdc.cam.ac.uk).

[8] Variable temperature magnetic measurements were made using a SQUID magnetometer (Quantum Design) with samples sealed in gelatin capsules in a field of 1000 Oe.

[9] J. J. Borrás-Almenar, J. M. Clemente-Juan, E. Coronado, B. S. Tsukerblat, *Inorg. Chem.* **1999**, *38*, 6081 – 6088.

[10] a) M. A. Halcrow, J.-S. Sun, J. C. Huffman, G. Christou, *Inorg. Chem.* **1995**, *34*, 4167 – 4177; b) K. S. Murray, *Adv. Inorg. Chem.* **1996**, *43*, 322.

[11] I. D. Brown, D. Altermatt, *Acta Crystallogr. Sect. B* **1985**, *41*, 244 – 247.

Synthesis of a Cyclopropene Analogue of Ceramide, a Potent Inhibitor of Dihydroceramide Desaturase**

Gemma Triola, Gemma Fabriàs,* and Amadeu Llebaria*

Dedicated to Professor Francisco Camps

Ceramide is a biologically relevant sphingolipid, which is intracellularly generated by either the breakdown of glycosphingolipids, the hydrolysis of sphingomyelin (sphingomyelin pathway), or the de novo biosynthesis (Scheme 1).[1] Despite the general acceptance of ceramide as a key second messenger, some aspects of ceramide-mediated signal transduction are controversial. The selective inhibition of the different enzymes involved in the biosynthesis and metabolism of ceramide can help solve such discrepancies and to better understand the precise role of ceramide in cell biology. This fact has led to the discovery of several inhibitors of these enzymes.[1–3]

The de novo biosynthetic pathway of ceramide (Scheme 1) is initiated with the condensation of palmitoyl CoA with serine to give 3-ketosphinganine, which is transformed into dihydroceramide upon reduction and acylation. The last step involves the introduction of the C4–C5 *trans* double bond into dihydroceramide to give ceramide. This reaction is catalyzed by dihydroceramide desaturase, for which no inhibitor has been reported previously.[4]

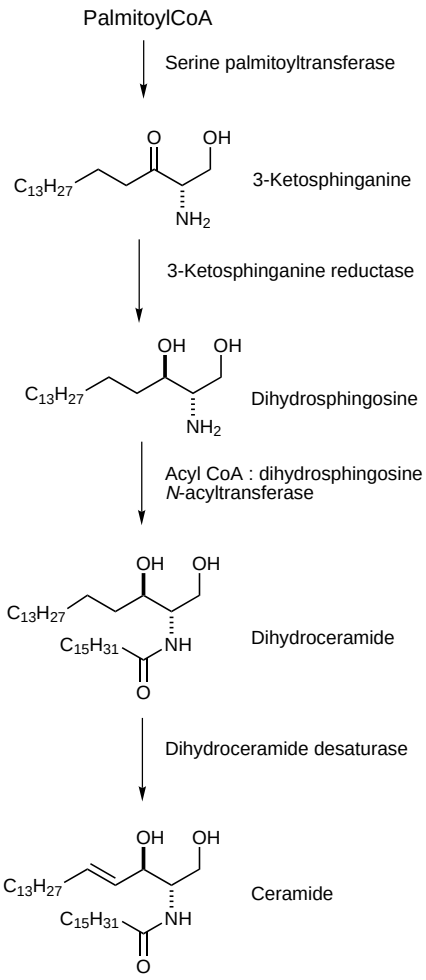

Scheme 1. De novo biosynthesis of ceramide.

Although little information is available about dihydroceramide desaturase,[5–10] it appears to be similar to the better known fatty acyl desaturases. After early reports on the activity of sterculic acid (9,10-methyleneoctadec-9-enoic acid) as a potent inhibitor of the Δ^9 stearoyl-CoA desaturase,[11] the inhibitory effect of cyclopropene fatty acids on different acyl-CoA desaturases has been the subject of several publications.[12] Although the mechanism of inhibition is still controversial,[12] it is well established that a) sterculic acid inhibits the Δ^9 desaturation of different aliphatic acids, regardless of the chain length;[13] b) among several synthetic cyclopropene fatty acids, only those compounds with the ring at C9 and/or C10 are effective inhibitors of the Δ^9 desaturase;[14] and c) a structural analogue of sterculic acid with an exocyclic double bond does not inhibit the desaturation of stearic to oleic acid.[15]

In light of these reports, the cyclopropene-containing ceramide *erythro*-**1** was designed as a putative inhibitor of dihydroceramide desaturation. We describe herein the synthesis of cyclopropene ceramide analogue *erythro*-**1**, as well as inhibition experiments that show that *erythro*-**1** is a potent inhibitor of dihydroceramide desaturase.

[*] Dr. G. Fabriàs, Dr. A. Llebaria, G. Triola
Department of Biological Organic Chemistry (IIQAB-CSIC)
Jordi Girona 18-26, 08034-Barcelona (Spain)
Fax: (+34) 93-2045904
E-mail: gfdqob@cid.csic.es, alsqob@cid.csic.es

[**] This work was supported by the Dirección General de Enseñanza Superior e Investigación Científica (grant PB97-1171) and the Departament d'Universitats, Recerca i Societat de la Informació, Generalitat de Catalunya (grant 1999-SGR 00187 and a Predoctoral fellowship to G.T.). We thank Dr. J. Casas, Dr. A. Delgado, and Dr. J. Joglar for their help in different aspects of this work.

  0044-8249/01/11310-2014 $ 17.50+.50/0